Published in final edited form as:
Cytoskeleton (Hoboken). 2012 July ; 69(7): 496–505. doi:10.1002/cm.21016.

Repulsive axon guidance cues ephrin-A2 and slit3 stop protrusion of the growth cone leading margin concurrently with inhibition of ADF/cofilin and ERM proteins

Bonnie M. Marsick[†], **Florence K. Roche**, and **Paul C. Letourneau**[*]
Department of Neuroscience, 6-145 Jackson Hall, 321 Church St SE University of Minnesota, Minneapolis, MN 55455

Abstract

Axonal growth cones turn away from repulsive guidance cues. This may start with reduced protrusive motility in the region the growth cone leading margin that is closer to the source of repulsive cue. Using explants of E7 chick temporal retina, we examine the effects of two repulsive guidance cues, ephrin-A2 and slit3, on retinal ganglion cell growth cone protrusive activity, total F-actin, free F-actin barbed ends, and the activities (phosphorylation states) of actin regulatory proteins, ADF/cofilin and ERM proteins. Ephrin-A2 rapidly stops protrusive activity simultaneously with reducing F-actin, free barbed ends and the activities of ADF/cofilin and ERM proteins. Slit3 also stops protrusion and reduces the activities of ADF/cofilin and ERM proteins. We interpret these results as indicating that repulsive guidance cues inhibit actin polymerization and actin-membrane linkage to stop protrusive activity. Retrograde F-actin flow withdraws actin to the C-domain, where F-actin bundles interact with myosin II to generate contractile forces that can collapse and retract the growth cone. Our results suggest that common mechanisms are used by repulsive guidance cue to disable growth cone motility and remodel growing axon terminals.

Keywords

actin dynamics; P-domain; F-actin

Introduction

Elongating axons are guided to their targets by attractive and repulsive guidance cues that induce growth cone turning. Changes in the dynamics of the growth cone leading margin, called the peripheral (P-) domain, initiate growth cone turning (Dent et al., 2010). Attractive turning involves local increases in F-actin networks, membrane expansion and adhesive interactions that advance the P-domain toward a cue, while repulsive turning involves opposite changes in the P-domain. One focus of the intracellular signaling that regulates growth cone turning is actin filament dynamics and organization in the P-domain (Gallo and Letourneau, 2004). Much remains unclear about the roles of actin regulatory proteins in controlling actin organization during attractive and repulsive growth cone turning (Pak et al., 2008).

Attractive growth cone turning involves increased F-actin in the P-domain region that is closer to the attractant (Marsick et al., 2010). This involves actin polymerization through activation of Rac1 and Cdc42 GTPases (Bashaw and Klein, 2010; Dent et al., 2010).

[*]Corresponding author: Paul C Letourneau; letou001@umn.edu.
[†]Current address: The Scripps Research Institute, La Jolla CA 92037

Attractive cues NGF and netrin increase activities of the actin severing protein, ADF/cofilin, and the anti-capping protein, Ena/Vasp (Dent et al., 2010; Evans et al., 2006; Marsick et al., 2010; Pak et al., 2008). Stimulation of these proteins increases F-actin barbed ends that are available for actin polymerization. The actin filament-membrane linker proteins, ERMs (ezrin, radixin, moesin), are also activated by neurotrophins and by netrin (Antoine-Bertrand et al., 2011; Marsick et al., 2012; McClatchey and Fehon, 2009). The combined activation of these actin regulatory proteins at the leading edge promotes local actin polymerization and membrane linkage that protrudes the P-domain toward an attractive cue.

The effects of repulsive cues on protrusion may be opposite those of attractive cues. Fan et al. (1993) reported that the first described repulsive cue, Semaphorin3A, (Sema3A) stopped protrusion of the leading margin of sensory (DRG) growth cones. Cessation of protrusion was also reported for *Xenopus* retinal growth cones exposed to ephrin-A1 (Woo et al., 2009). In contrast to the effects of NGF and netrin, studies report that Sema3A induces phosphorylation changes that inactivate ADF/cofilin and ERM proteins (Aizawa et al., 2001; Gallo, 2008; Mintz et al., 2008). Because these studies were conducted in different laboratories, it is unclear how the changes in these actin regulatory proteins are involved in Semphorin3A-induced cessation of leading edge protrusion. In addition, understanding the actions of repulsive cues is complex, as repellent cues often induce profound responses than involve activities beyond the P-domain, such as collapse of growth cones, activation of myosin II, and retraction of the distal neurite or axon (Brown and Bridgman, 2009; Brown et al., 2009; Gallo, 2006; Gallo and Letourneau, 2004).

Ephrin-A ligands are surface-bound repulsive cues that guide axonal patterning in multiple systems (Feldheim and O'Leary, 2010; Kolodkin and Tessier-Lavigne, 2010). In this study we investigated the effects of ephrin-A2 on leading edge protrusion, F-actin content, free F-actin barbed ends, and phosphorylation of ADF/cofilin and ERM proteins in growth cones of chick temporal retinal ganglion cells. Our results indicate a concurrent loss of protrusive activity, F-actin, free actin barbed ends and activities of ADF/cofilin and ERM. Together with data using the repellent slit3, our results suggest that repulsive growth cone turning involves common activities that block leading edge protrusion through inhibition of actin polymerization and F-actin/plasma membrane linkages.

Results

The *in vitro* responses of temporal retinal ganglion cell growth cones to the global addition of ephrin-A2 can involve several context-dependent morphological transformations. The initial response is cessation of the protrusion of the growth cone leading margin, which may be followed by extensive collapse and retraction of the growth cone and distal axon. Retraction engages the growth cone body and distal axon in an actomyosin-powered contraction that ruptures adhesions and compresses the growth cone and axonal cytoskeleton. In this study we cultured temporal retinal explants on substrates of L1 CAM. Retinal growth cones spread broadly on L1 CAM and axons adhere to L1. This adhesive substrate slows retraction, allowing analysis of the initial effects of ephrin-A2 on growth cone protrusion and actin organization. When these neurons are cultured on a laminin-coated substratum, the same ephrin-A2 treatment often produces extensive growth cone collapse and axonal retraction.

Ephrin A treatment stops growth cone protrusion

Kymograph analysis of phase contrast imaging of growth cone leading edges at 3 sec intervals was conducted to visualize the effects of ephrin-A2 on protrusion of the growth cone leading margin. The kymographs show transient protrusions and withdrawals, as well as a net advance of the leading margin before adding ephrin-A2 (Figure 1; Movie S1 in

supplementary material). However, when 0.5 or 2 μg/ml ephrin-A2 was added to the culture medium, protrusion of the leading margin ceased within 5 min or less, producing a nearly flat line kymograph without subsequent protrusion of the growth cone leading margin.

Ephrin-A2 treatment reduces F-actin content and changes the distribution of F-actin

The rapid cessation of growth cone protrusion following ephrin-A2 treatment is related to the reduced F-actin content reported in growth cones of neurons treated with ephrin-A2 (Gallo et al., 2002; Roche et al, 2009). To characterize the reduced F-actin content after ephrin-A2 treatment, retinal neuronal explants were fixed after 0, 1, 2, 5, 10 and 15 min of ephrin-A2 treatment for staining with fluorescent phalloidin and determination of F-actin content and distribution. Figure 2A illustrates phalloidin staining of typical growth cones at several time points after adding ephrin-A2. Quantification of growth cone phalloidin staining indicated that total integrated F-actin in growth cones was significantly reduced by 2 min of ephrin-A2 treatment and remained reduced over the 15 min of ephrin-A2 treatment (Fig. 2B). Figure 2C shows the ephrin-A2-induced loss of F-actin was greater in growth cone P-domains than the C-domains (Fig. 2A'), and the relative F-actin distribution shifted more centrally within minutes of adding ephrin-A2. Thus, ephrin-A2 treatment led to a rapid loss of F-actin at the growth cone peripheral margin, while the F-actin content of the central domain was less reduced.

Ephrin-A2 treatment does not increase retrograde actin flow

An increase in F-actin retrograde flow could contribute to the loss of F-actin from the growth cone leading margin after ephrin-A2 treatment. Ephrin-A2 signaling increases Rho kinase activity, which could accelerate retrograde flow through activation of myosin II (Wahl et al., 2000). We analyzed retrograde actin flow by visualizing GFP-ß-actin in transfected retinal ganglion cell growth cones before and after addition of ephrin-A2. Kymograph analysis (images not shown) revealed that the mean rate of retrograde actin flow at the growth cone leading margin of growth cones was 9.6 ± 0.8 μm/min before adding ephrin-A2, similar to our previous determinations (Marsick et al., 2010). At 5 min after adding ephrin-A2 the rate of retrograde actin flow was not significantly increased compared to before adding ephrin-A2 (10.2 ± 1.4 μm/min; n=5). Thus, increased F-actin retrograde flow from the growth cone leading margin does not significantly contribute to the ephrinA2-induced cessation of growth cone protrusion.

Ephrin-A2 treatment reduces F-actin free barbed ends

Another source of the ephrin-A2-induced loss of F-actin at the growth cone leading margin may be inhibition of actin polymerization. We used an assay for labeling F-actin free barbed ends in order to assess the effects of ephrin-A2 treatment on the quantity and location of F-actin free barbed ends, which are sites of actin polymerization (Marsick et al., 2010). Retinal explant cultures were permeabilized and briefly incubated with rhodamine-actin at 1, 5, and 10 min after addition of ephrin-A2. After even one min of ephrin-A2 treatment F-actin barbed ends at the growth cone leading margin were significantly reduced, and this reduction remained for 10 min of ephrin-A2 treatment (Fig. 3A). As we did previously in analyzing the reduced F-actin content of ephrinA2-treated growth cones, we divided the fluorescence images of rhodamine-actin incorporation into peripheral and central compartments (Fig. 2A'). As seen in Figure 3B, the reduction in F-actin barbed ends was greater in the growth cone periphery than in the central growth cone region.

Ephrin-A2 treatment increases ADF/cofilin phosphorylation and decreases ERM phosphorylation

In previous studies of attractive guidance cues, we found that coordinated activation of two actin regulatory proteins, ADF/cofilin and ERM, may mediate the increased growth cone protrusion that initiates a growth cone turn towards a source of attractive cue. Several studies with Sema3A showed that ADF/cofilin and ERM proteins are transiently inactivated after treating sensory neuronal cultures (Aizawa et al., 2001; Gallo, 2008; Mintz et al., 2008). Therefore, we examined the effects of ephrin-A2 treatment on the phosphorylation states of ADF/cofilin (P-ADF/cofilin is inactive) and ERM proteins (P-ERM is active) with attention to the temporal relationship of these protein activities to the dynamics of ephrin-A2-induced inhibition of growth cone protrusion and actin dynamics.

To assess the effects of ephrin-A2 on ADF/cofilin and ERM activity temporal retinal explants were fixed and stained with fluorescent phalloidin and anti-P-cofilin or anti-P-ERM following 1-15 min treatment with ephrin-A2. As shown in Figure 4A, the mean intensity of growth cone staining for P-cofilin was significantly elevated following 5 min treatment with ephrin-A2. This increase in P-cofilin had diminished by ten min ephrin-A2 treatment. This finding of a transient elevation of mean growth cone P-cofilin staining is similar to a previous report on the effects of Sema3A on DRG neuronal growth cones (Aizawa et al., 2001). Thus, exposure to ephrin-A2 caused increased phosphorylation of ADF/cofilin, which is consistent with a reduced activity of ADF/cofilin and reduced actin dynamics. As shown in Figure 4B, the mean intensity of growth cone staining for P-ERM was also decreased by just one min ephrin-A2 treatment, and remained reduced for at least 15 min of ephrin-A2 treatment. This reduced ERM phosphorylation after adding ephrinA2 is consistent with previous studies with Sema3A (Gallo, 2008; Mintz et al., 2008). Together, these data indicate that ephrin-A2 treatment rapidly reduces both ADF/cofilin and ERM activities prior to and/or during the loss of P-domain F-actin.

Ephrin-A2 effects on actin-related motility are similar to those of cytochalasin D

The ephrin-A2-induced cessation of protrusion and loss of F-actin from the growth cone leading margin resembles the action of the drug cytochalasin D, which stops actin polymerization by capping F-actin barbed ends. To compare the effects of cytochalasin D and ephrin-A2, we made kymographs of leading edge protrusion and also visualized retrograde actin flow in growth cones of retinal neurons transfected to express GFP-ß-actin. As expected, ephrin-A2 and cytochalasin D both rapidly stopped protrusion of the growth cone leading margin (Fig. 5A; Movies S2 and S3 in supplementary material). Addition of cytochalasin D did not halt retrograde flow, and in combination with the cessation of actin polymerization, the retrograde flow removed F-actin from the leading cell margin, except for a thin subplasmalemmal actin cortex (Fig. 5B). In similar manner, visualization of retrograde actin flow after addition of ephrin-A2 showed loss of actin from the growth cone leading margin, as ephrin-A2 signaling inhibited actin polymerization at the leading margin (Fig. 5C).

Slit3 similarly regulates protrusion, ADF/cofilin and ERM phosphorylation in retinal growth cones

Slits are secreted glycoproteins with several developmental roles, including as axonal chemorepellents for growth cones of retinal ganglion cells (Plachez et al., 2008; Thompson et al., 2009). We investigated the effects of Slit3 on the protrusive activity of retinal ganglion cell growth cones and on the phosphorylation of ADF/cofilin and ERM proteins. Similar to the effects of ephrin-A2 on growth cones of temporal retinal growth cones, slit3 induces a rapid cessation of growth cone protrusion, an increase in ADF/cofilin

phosphorylation, and a decrease in ERM phosphorylation (Fig. 6; Movie S4 in supplementary material).

Discussion

We previously found that growth cone turning to attractive cues involves activation of actin regulatory proteins ADF/cofilin and ERM (ezrin, radixin, moesin) proteins to stimulate localized actin polymerization, membrane protrusion and turning of the leading margin toward an attractant (Marsick et al., 2010, 2011). In this study we investigated the effect of repulsive guidance cues, ephrin-A2 and slit3, on protrusion of retinal ganglion cell growth cone leading margin and on ADF/cofilin and ERM protein activities. Ephrin-A2 has opposite effects than attractive cues, rapidly inhibiting growth cone protrusion, and at the same time reducing F-actin content, free F-actin barbed ends, and the activity states of ADF/cofilin and ERM proteins in growth cone leading margins. Slit3 had similar effects on growth cone protrusion and on phosphorylation states of ADF/cofilin and ERM proteins. The similarity of these results to studies with Sema3A suggest common mechanisms exist by which repulsive guidance cues disable the actin machinery at the leading margin.

Protrusion of the growth cone leading margin involves 3 activities, expansion of the plasma membrane, formation of substrate adhesions and advancing actin filament assembly. Signaling by repulsive cues Sema3A and ephrin-A2 limits the first two of these activities by increasing plasma membrane endocytosis and by preventing new substrate adhesions (Bechara et al., 2008; de La Houssaye et al., 1999; Jurney et al., 2002; Kabayama et al., 2009; Kolpak et al., 2009; Woo et al., 2009). We found that ephrin-A2 signaling decreased total F-actin and incorporation of rhodamine-actin onto F-actin free barbed ends in the P-domain. Because the rate of retrograde F-actin flow was not altered by ephrin-A2, our results suggest that decreased actin polymerization and/or increased depolymerization account for the ephrin-A2-induced F-actin loss.

Although ADF/cofilin severs F-actin and destabilizes F-actin pointed ends, the role of ADF/cofilin in regulating F-actin in the P-domain is poorly understood. ADF/cofilin is activated by attractants NGF and netrin, as F-actin severing at the leading edge creates more actin barbed ends to increase actin polymerization and protrusion (Gehler et al., 2004; Marsick et al., 2010). Conversely, ADF/cofilin inactivation by ephrin-A2, slit3 and Sema3A may reduce actin barbed ends at the leading margin and decrease actin polymerization. In addition, inhibition of ADF/cofilin by repulsive cues may decrease F-actin turnover in the C-domain, which may increase the actin network that undergoes actomyosin contractility to mediate repellent-induced growth cone collapse and retraction. We previously showed that reducing F-actin turnover in growth cones pharmacologically is sufficient to induce growth cone and axon retraction (Gallo et al., 2002).

As ephrin-A2 stops actin polymerization, retrograde actin flow withdraws the actin network from the leading margin. These events are similar to the effects of cytochalasin D, which blocks actin polymerization (as also noted by Fan et al., 1993). Both treatments rapidly stop protrusion, and kymography of YFP-actin-expressing growth cones subjected to either cytochalasin D or ephrin-A2 showed retreat of F-actin from the leading margin, as the retrogradely moving F-actin was not replaced by polymerization at the leading margin. Repulsive cues may further suppress protrusion via actin depolymerization through the redox enzyme Mical, which destabilizes actin filaments (Hung et al., 2010). However, actin depolymerization occurs predominantly in the transition zone or C-domain, not at the leading edge (Medeiros et al., 2006), so the loss of F-actin in the leading margin is most likely due to inhibition of actin polymerization.

Concurrent with the inactivation of ADF/cofilin, ephrin-A2 and slit3 signaling suppress the activity of ERMs, similar to the effects of Sema3A (Gallo, 2008; Mintz et al., 2008). ERM inactivation may contribute in several ways to inhibiting growth cone protrusion. Loss of ERM-mediated actin-membrane linkage facilitates the withdrawal of F-actin by retrograde actin flow. The neuronal adhesion protein L1 is a major binding partner for ERM proteins in the growth cone P-domain, and the decrease in ERM-L1 binding may increase the endocytic removal of L1 from filopodia and the P-domain, which would contribute to the reduced adhesion at the leading margin. Finally, ERM inactivation may disassemble scaffolds for signaling and adaptor proteins, such as PKA and EPAC, which regulate cytoskeletal and adhesive functions. In a prior paper we suppressed ERM function in growth cones with a dominant negative ERM construct (Marsick et al., 2012). In several ways these growth cones resembled growth cones exposed to repulsive guidance cues. Total growth cone F-actin and F-actin free barbed ends at the leading margin were reduced when ERMs were inhibited, as was filopodial expression of L1. In addition, as discussed below, inhibition of ERM function resulted in a greater fraction of F-actin being located in the growth cone C-domain. Thus, inhibition of ERM function is also a component of the loss of protrusive activity, as a growth cone turns away from a repulsive cue.

Although ephrin-A2 treatment reduces total F-actin in growth cones, the F-actin reduction is greater in the P-domain that in the growth cone center. F-actin bundles persist in the C-domain of ephrin-A2 treated growth cones (Fig. 2) (Roche et al., 2009), and as we previously reported, these bundles are more stable than F-actin arrays in control growth cones (Gallo et al., 2002). Changes in the location and activities of several actin regulatory proteins coordinate this actin filament reorganization (Brown and Bridgman, 2009; Gallo, 2006). These F-actin bundles in the growth cone C-domain and the terminal axon undergo contraction with RhoA-activated myosin II to retract growth cones and terminal axonal segments (Brown and Bridgman, 2009; Brown et al., 2009; Gallo, 2006). These contractile events are a second phase of the repulsive responses that steer growth cones away from negative guidance cues. In addition, growth cone and axonal retraction may drive the pruning of axonal branches during the refinement of synapses within target regions (Chacon et al., 2010; Tran et al., 2007; Vanderhaeghen and Cheng, 2010).

The intracellular signaling from repulsive guidance cues that mediates inhibition of growth cone protrusive activity is not well understood. One feature of repulsive guidance signaling that is common to Sema3A, ephrin-A2 and slits is involvement of the Rho GTPases RhoA and Rac1 (Bashaw and Klein, 2011; Jurney et al., 2002; Wahl et al., 2000). RhoA activity increases ADF/cofilin phosphorylation via LIM kinase, resulting in reduced F-actin barbed ends and reduced actin polymerization. The GTPase Rac1 mediates endocytosis of the plasma membrane to further reduce protrusive activity. In the case of ephrin-A signaling, the guanine nucleotide exchange factor ephexin activates RhoA (Shamah et al., 2001), while ephrin-A-mediated inhibition of another GTPase, Rheb, also contributes to growth cone collapse (Nie et al., 2010). The mechanisms of ERM de-phosphorylation in repulsive cue signaling are poorly understood. Sema3A-induced loss of ERM phosphorylation occurs by inhibition of PI3 kinase (Gallo, 2008). However, ERM phosphorylation is mediated by several kinases (Antoine-Bertrand et al., 2011; Marsick et al., 2012). Ephrin-A-induced growth cone collapse involves the activities of several cytoplasmic kinases src, FAK, and Abelson kinase (Harbotta and Nobes, 2005; Knoll and Drescher, 2004; Wahl et al., 2000; Woo et al., 2009). Thus, it remains a mystery what repulsive signals mediate the de-phosphorylation of ERM proteins. Furthermore, cessation of growth cone protrusion may also involve inhibition of other regulatory proteins that promote actin polymerization, such as formins, Ena/VASP and the Arp2/3 complex (Dent et al., 2010).

In summary, treatment of temporal retinal explants with ephrin-A2 or slit3 stops protrusion of growth cone leading margins and concurrently reduces the activities of actin regulatory proteins, ADF/cofilin and ERM proteins. These changes suppress actin polymerization and facilitate the retrograde removal of F-actin from the leading margin. Similar events are reported for another repulsive cue, Sema3A, indicating that repulsive guidance cues may share common mechanisms to suppress protrusion of the leading margin and initiate growth cone turning away from repulsive cues. Work is needed to further clarify the complex signaling events and the changes in actin regulatory proteins that are involved in growth cone repulsion and remodeling of axon terminals.

Materials and Methods

Materials

F-12 medium, B27 additives, poly-D-lysine (MW >300,000), Alexa Fluor 488- and 568–phalloidin, Alexa Fluor 488- and 568- secondary antibodies were purchased from Invitrogen. Ephrin-A2, Slit3, and L1-Fc were purchased from R & D Systems. White leghorn fertilized chicken eggs were purchased from Hy-Line North America, LLC. All other reagents were purchased from Sigma-Aldrich, unless otherwise indicated.

Neuronal culture

Glass coverslips (Gold Seal) were coated with 100ug/ml poly-D-lysine, rinsed three times with water, dried, coated with 5% nitrocellulose dissolved in 100% amyl acetate (Fischer Scientific), dried, and coated overnight with 4μg/ml L1-Fc in phosphate buffered solution (PBS; Roche). For videomicroscopy video dishes were made by gluing (silicone aquarium sealant) a coverslip (18 mm × 18 mm; Gold Seal) over a hole (5mm) in the bottom of a culture dish (Falcon 35 mm × 10 mm), allowed to dry, rinsed with water, and coated with L1-Fc. Embryonic day 7 (E7) temporal retinal explants were dissected from chick embryos of either sex, according to procedures approved by the University of Minnesota Institutional Animal Care and Use Committee. Retinal explants were cultured on experimental substrates in F-12 with added B27, glutamine, sodium pyruvate and glucose, and buffered to pH 7.4 with 10 mM HEPES. Neural tissues were cultured overnight in a humidified incubator at 37°C.

Videomicroscopy and Kymograph Analysis

E7 retinal explants were cultured 24 h, on L1-coated video dishes. A growth cone was selected, and imaged at 3-5s intervals, using an Olympus IX70 inverted microscope with a 60X oil immersion lens. When a guidance cue was added, a black frame was captured to mark the time of addition (seen as a black line in the kymograph). After the recording was finished and saved, the video sequence was opened in ImageJ and a one pixel-wide line was drawn forward from the axis of the terminal axonal segment. Using the “stacks → reslice” function, a kymograph was generated and enlarged for better visualization.

Immunocytochemistry

Neuronal cultures were fixed and blocked as described in Roche et al. (2009). Coverslips were incubated with primary antibodies diluted in PBS containing 10% goat serum overnight at 4° C. Antibody 4321 (against phospho-ADF/cofilin) was used at 1:1000 (generous gift of Dr. James R. Bamburg, Colorado State University, Fort Collins, CO), Anti phospho-ERM (Cell Signaling Technology) was used at 1:50. Coverslips were then rinsed 3 times in PBS and incubated in PBS rinse for 1 h. For labeling F-actin, Alexa Fluor 488–phalloidin was applied at a 1:20 dilution, and mixed with secondary antibodies: Alexa Fluor

568 goat anti-rabbit at 1:1000 dilution in PBS with 10% goat serum for 1 h. After rinsing 3 times in PBS, coverslips were mounted in *SlowFade* reagent (Invitrogen).

Quantitative fluorescence determinations

A Spot digital camera mounted on an Olympus XC-70 inverted microscope, and MetaMorph software (Molecular Devices) were used for all image acquisitions. In any one experiment, all fluorescence images were acquired in one session. For repeat experiments, data were normalized to controls. For collection of fluorescent images, exposure time and gain settings on the digital camera were kept constant, and image acquisition and analysis was performed as described in Roche et al. (2009).

For experiments measuring growth cone fluorescence intensity values of phalloidin, Rhodamine-actin and P-ADF/cofilin labeling, a line tool in MetaMorph was used to outline the terminal 25 μm of each distal axon and growth cone, and background intensity value was subtracted from the fluorescence intensity value of the accompanying neuronal measurement. For phospho-ERM intensity measurements, growth cones were selected at random from phalloidin images and a 3 μm wide line was drawn to trace the leading growth cone margin using the line tool. The lines were then transferred to the corresponding phospho-ERM image and background-subtracted intensity values were recorded.

Central and peripheral region quantifications of total F-actin and barbed labeling were performed by hand-tracing fluorescent phalloidin images in Metamorph. A straight line was then drawn across the growth cone width in at least 3 locations and the distance 25% from either side of the growth cone edge was noted and used to trace a central growth cone region. Regions were then transferred to the F-actin or rhodamine-actin images, where total and central growth cone intensities were measured. Peripheral growth cone intensities were later calculated by subtracting the central intensity from the total for each growth cone.

Retrograde flow measurements

To determine retrograde actin flow rates, neurons were transfected to express GFP-ß-actin, and cultured overnight, as described in Marsick et al. (2011). Transfected growth cones were identified, and GFP-actin was imaged every 3 s for 6-10 min. Kymographs were generated for the distal 10 μm of growth cones, and flow rates were measured by tracking bright GFP-actin features, which are formed by unequal incorporation of GFP- and non-GFP-actin monomers into polymerized filaments at the leading edge. Measuring retrograde flow using the movement of these features has been described previously (Marsick et al., 2010), including a demonstrated sensitivity of this retrograde flow to the myosin-II inhibitor blebbistatin (Chan and Odde, 2008).

Barbed end labeling

This protocol was adapted from Chan et al. (1998) and is described in Marsick et al. (2010).

Supplementary Material

Refer to Web version on PubMed Central for supplementary material.

Acknowledgments

This research was supported by grants from the NIH (HD19950-22) and from the Minnesota Medical Foundation.

References

Aizawa H, Wakatsuki S, Ishii A, Moriyama K, Sasaki Y, Ohashi K, Sekine-Aizawa Y, Sehara-Fujisawa A, Mizuno K, Goshima Y, Yahara I. Phosphorylation of cofilin by LIM kinase is necessary for semaphorin3A-induced growth cone collapse. Nature Neuro. 2001; 4:367–73.

Antoine-Bertrand J, Ghogha A, Luangrath V, Bedford FK, Lamarche-Vane N. The activation of ezrin-radixin-moesin proteins is regulated by netrin-1 through Src kinase and RhoA/Rho kinase activities and mediates netrin-1-induced axon outgrowth. Mol Biol Cell. 2011; 22:3734–46. [PubMed: 21849478]

Bashaw GJ, Klein R. Signaling from axon guidance receptors. Cold Spring Harb Perspect Biol. 2010; 2:a001941. published online March 24, 2010. [PubMed: 20452961]

Bechara A, Nawabi H, Moret F, Yaron A, Weaver E, Bozon M, Abouzid K, Guan JL, Tessier-Lavigne M, Lemmon V, Castellani V. FAK-MAPK-dependent adhesion disassembly downstream of L1 contributes to semaphorin3A-induced collapse. EMBO J. 2008; 27:1549–62. [PubMed: 18464795]

Brown JA, Bridgman PC. Disruption of the cytoskeleton during Semaphorin 3A induced growth cone collapse correlates with differences in actin organization and associated binding proteins. Dev Neurobiol. 2009. 2009; 69:633–46.

Brown JA, Wysolmerski RB, Bridgman PC. Dorsal root ganglion neurons react to Semaphorin 3A application through a biphasic response that requires multiple Myosin II isoforms. Mol Biol Cell. 2009; 20:1167–79. [PubMed: 19109430]

Chacon MR, Fernandez G, Rico B. Focal adhesion kinase functions downstream of Sema3A signaling during axonal remodeling. Mol Cell Neurosci. 2010; 44:30–42. [PubMed: 20159040]

Chan AY, Raft S, Bailly M, Wyckoff JB, Segall JE, Condeelis JS. EGF stimulates an increase in actin nucleation and filament number at the leading edge of the lamellipod in mammary adenocarcinoma cells. J Cell Sci. 1998; 111:199–211. [PubMed: 9405304]

Chan CE, Odde DJ. Traction dynamics of filopodia on compliant substrates. Science. 2008; 322:1687–91. [PubMed: 19074349]

de La Houssaye BA, Mikule K, Nikolic D, Pfenninger KH. Thrombin-induced growth cone collapse: involvement of phospholipase A(2) and eicosanoid generation. J Neurosci. 1999; 19:10843–55. [PubMed: 10594066]

Dent EW, Gupton SL, Gertler FB. The growth cone cytoskeleton in axon outgrowth and guidance. Cold Spring Harb Perspect Biol. 2010 doi: 10.1101/cshperspect.a001800.

Drescher U, Kremoser C, Handwerker C, Löschinger J, Noda M, Bonhoeffer F. In vitro guidance of retinal ganglion cell axons by RAGS, a 25 kDa tectal protein related to ligands for Eph receptor tyrosine kinases. Cell. 1995; 82:359–70. [PubMed: 7634326]

Evans IR, Renne T, Gertler FB, Nobes CD. Ena/VASP proteins mediate repulsion from ephrin ligands. J Cell Sci. 2006; 120:289–98. [PubMed: 17179204]

Fan J, Mansfield SG, Redmond T, Gordon-Weeks PR, Raper JA. The organization of F-actin and microtubules in growth cones exposed to a brain-derived collapsing factor. J Cell Biol. 1993; 121:867–78. [PubMed: 8491778]

Feldheim DA, O'Leary DDM. Visual map development: Bidirectional signaling, bifunctional guidance molecules and competition. Cold Spring Harb Perspect Biol. 2010; 2:a001768. 2010. [PubMed: 20880989]

Gallo G. RhoA-kinase coordinates F-actin organization and myosin II activity during semaphorin-3A-induced axon retraction. J Cell Sci. 2006; 119:3413–23. [PubMed: 16899819]

Gallo G. Semaphorin 3A inhibits ERM protein phosphorylation in growth cone filopodia through inactivation of PI3K. Dev Neurobiol. 2008; 68:926–33. [PubMed: 18327764]

Gallo G, Letourneau PC. Regulation of growth cone actin filaments by guidance cues. J. Neurobiology. 2004; 58:92–102.

Gallo G, Yee HF, Letourneau PC. Actin turnover is required to prevent axon retraction driven by endogenous actomyosin contractility. J. Cell Biol. 2002; 158:1219–28. [PubMed: 12356866]

Gehler S, Shaw AE, Sarmiere PD, Bamburg JR, Letourneau PC. Brain-derived neurotrophic factor regulation of retinal growth cone filopodial dynamics is mediated through actin depolymerizing factor/cofilin. J Neurosci. 2004; 24:10741–49. [PubMed: 15564592]

Hall A, Lalli G. Rho and Ras GTPases in axon growth, guidance, and branching. Cold Spring Harb Perspect Biol. 2010; 2:a001818. 2010. [PubMed: 20182621]

Harbotta LK, Nobes CD. A key role for Abl family kinases in EphA receptor-mediated growth cone collapse. Mol Cell Neurosci. 2005; 30:1–11. [PubMed: 15996481]

Hung RJ, Yazdani U, Yoon J, Wu H, Yang T, Gupta N, Huang Z, van Berkel WJ, Terman JR. Mical links semaphorins to F-actin disassembly. Nature. 2010; 463:823–7. [PubMed: 20148037]

Jurney WM, Gallo G, Letourneau PC, McLoon SC. Rac1 mediated endocytosis during ephrin-A2 and semaphorin 3A induced growth cone collapse. J Neurosci. 2002; 22:6019–28. [PubMed: 12122063]

Kabayama H, Nakamura T, Takeuchi M, Iwasaki H, Taniguchi M, Tokushige N, Mikoshiba K. Ca2+ induces macropinocytosis via F-actin depolymerization during growth cone collapse. Mol Cell Neurosci. 2009; 40:27–38. [PubMed: 18848894]

Knoll B, Drescher U. Src family kinases are involved in EphA receptor-mediated retinal axon guidance. J Neurosci. 2004; 24:6248–57. [PubMed: 15254079]

Kolodkin AL, Tessier-Lavigne M. Mechanisms and molecules of neuronal wiring: A Primer. Cold Spring Harb Perspect Biol. 2010; 3:a001727. 2011. [PubMed: 21123392]

Kolpak AL, Jiang J, Guo D, Standley C, Bellve K, Fogarty K, Bao Z-Z. Negative guidance factor-Induced macropinocytosis in the growth cone plays a critical role in repulsive axon turning. J Neurosci. 2009; 29:10488–98. [PubMed: 19710302]

Marsick BM, Flynn KC, Santiago-Medina M, Bamburg JR, Letourneau PC. Activation of ADF/cofilin mediates attractive growth cone turning toward nerve growth factor and netrin-1. Dev Neurobiol. 2010; 70:565–88. [PubMed: 20506164]

Marsick BM, San Miguel-Ruiz J, Letourneau PC. Activation of Ezrin/radixin/moesin mediates attractive growth cone guidance through regulation of growth cone actin and adhesion receptors. J Neurosci. 2012; 32:282–296. [PubMed: 22219290]

McClatchey AI, Fehon RG. Merlin and the ERM proteins--regulators of receptor distribution and signaling at the cell cortex. Trends Cell Biol. 2009; 19:198–206. [PubMed: 19345106]

Medeiros NA, Burnette DT, Forscher P. Myosin II functions in actin-bundle turnover in neuronal growth cones. Nat Cell Biol. 2006; 8:215–26. [PubMed: 16501565]

Mintz CD, Carcea I, McNickle DG, Dickson TC, Ge Y, Salton SR, Benson DL. ERM proteins regulate growth cone responses to Sema3A. J Comp Neurol. 2008; 510:351–66. [PubMed: 18651636]

Nie D, Di Nardo A, Han JM, Baharanyi H, Kramvis I, Huynh TT, Dabora S, Codeluppi S, Pandolfi Pasquale EB, Sahin M. Tsc2-Rheb signaling regulates EphA-mediated axon guidance. Nature Neurosci. 2010; 13:163–72. [PubMed: 20062052]

Niggli V, Rossy J. Ezrin/radixin/moesin: versatile controllers of signaling molecules and of the cortical cytoskeleton. Int J Biochem Cell Biol. 2008; 40:344–49. [PubMed: 17419089]

Pak CW, Flynn KC, Bamburg JR. Actin-binding proteins take the reins in growth cones. Nat Rev Neurosci. 2008; 9:136–47. [PubMed: 18209731]

Plachez C, Andrews W, Liapi A, Knoell B, Drescher U, Mankoo B, Zhe L, Mambetisaeva E, Annan A, Bannister L, Parnavelas JG, Richards LJ, Sundaresan V. Robos are required for the correct targeting of retinal ganglion cell axons in the visual pathway of the brain. Mol Cell Neurosci. 2008; 37:719–30. [PubMed: 18272390]

Roche FK, Marsick BM, Letourneau PC. Protein synthesis in distal axons is not required for growth cone responses to guidance cues. J. Neurosci. 2009; 29:638–52. [PubMed: 19158291]

Shamah SM, Lin MZ, Goldberg JL, Estrach S, Sahin M, Hu L, Bazalakova M, Neve RL, Corfas G, Debant A, Greenberg ME. EphA receptors regulate growth cone dynamics through the novel guanine nucleotide exchange factor ephexin. Cell. 2001; 105:233–44. [PubMed: 11336673]

Thompson H, Andrews W, Parnavelas JG, Erskine L. Robo2 is required for Slit-mediated intraretinal axon guidance. Dev Biol. 2009; 335:418–26. [PubMed: 19782674]

Tran TS, Kolodkin AL, Bharadwaj R. Semaphorin regulation of cellular morphology. Annu Rev Cell Dev Biol. 2007; 23:263–92. [PubMed: 17539753]

Vanderhaeghen P, Cheng H-J. Guidance molecules in axon pruning and cell death. Cold Spring Harb Perspect Biol. 2010; 2:a001859. 2010. [PubMed: 20516131]

Wahl S, Barth H, Ciossek T, Aktories K, Mueller BK. Ephrin-A5 induces collapse of growth cones by activating Rho and Rho kinase. J Cell Biol. 2000; 149:263–70. [PubMed: 10769020]

Woo S, Rowan DJ, Gomez TM. Retinotopic mapping requires focal adhesion kinase-mediated regulation of growth cone adhesion. J Neurosci. 2009; 29:13981–91. [PubMed: 19890008]

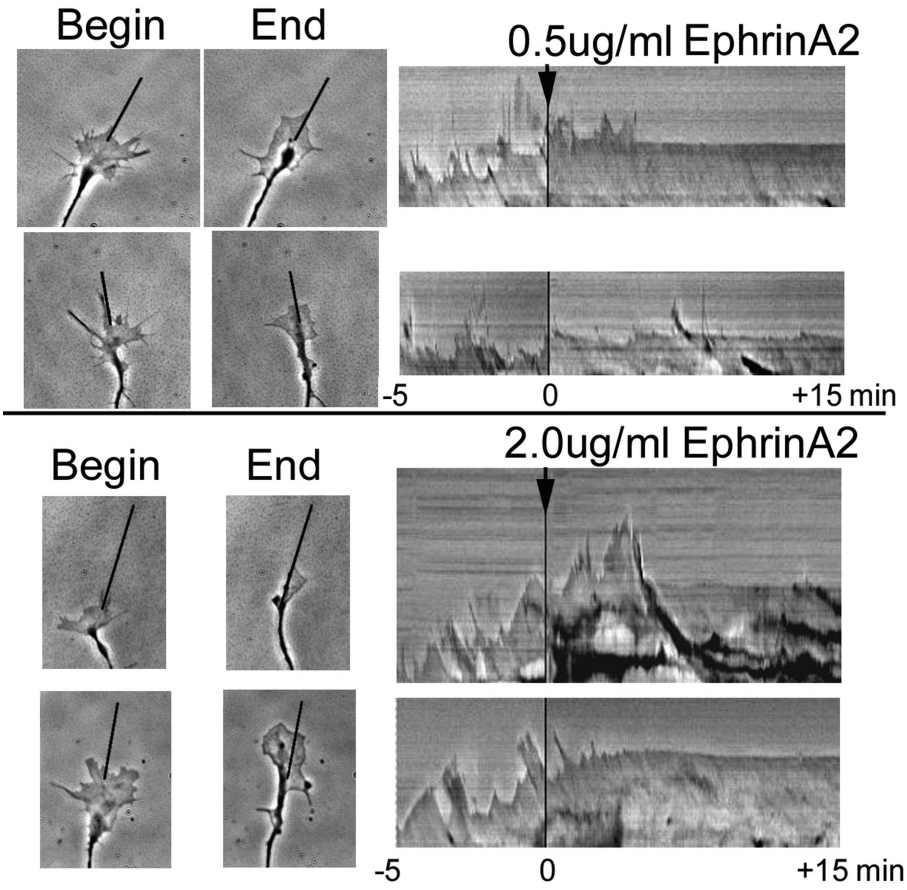

Figure 1.

Ephrin-A2 stops protrusion of the growth cone leading margin. Growth cones of temporal retinal ganglion cells were imaged every 5 sec for 5 min before and for 15 min after the addition of 0.5 μg/ml or 2.0 μg/ml ephrin-A2. Protrusive activity was stopped by 5 min after adding ephrin-A2. The kymographs shown at the right were generated from 1 μm wide slices taken along the indicated lines, which follow the axes of the terminal axon segments. Scale bar 10 μm.

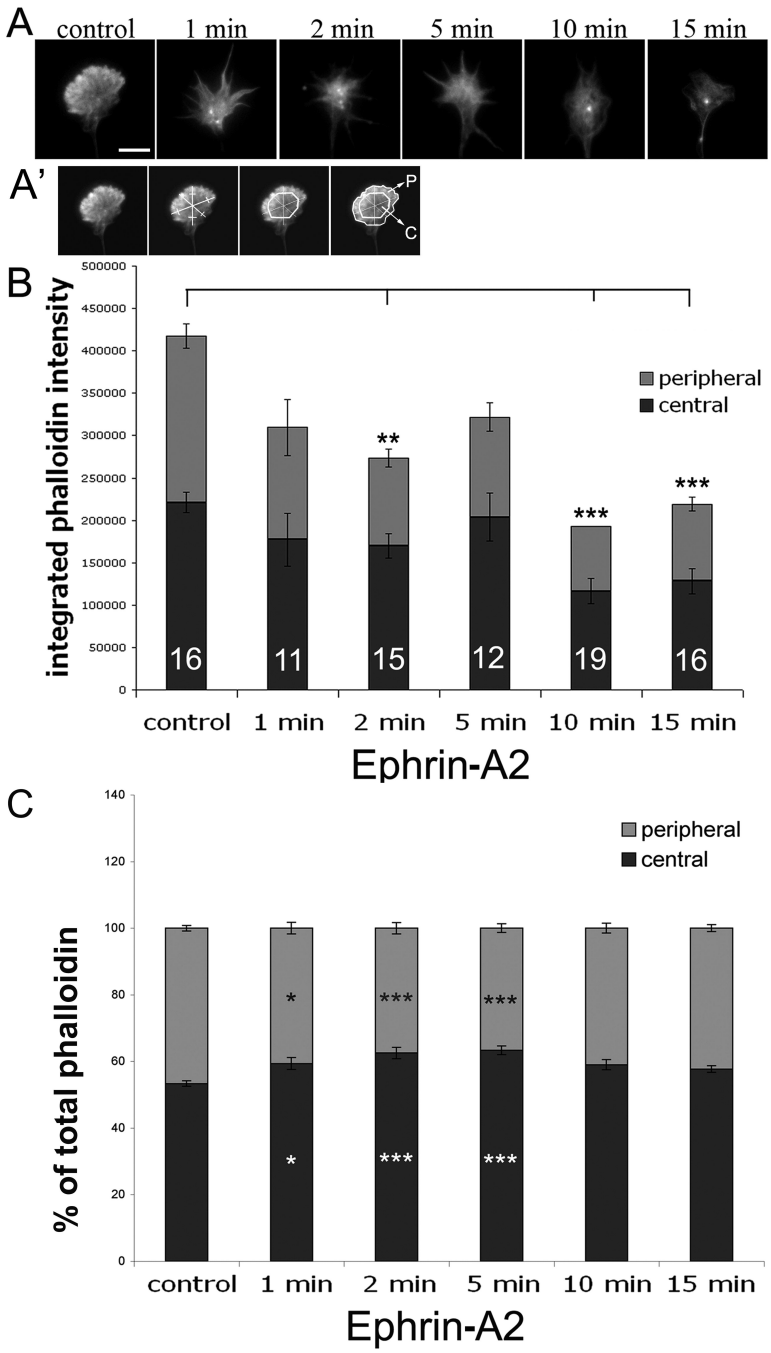

Figure 2.

Ephrin-A2 reduces total F-actin and shifts F-actin distribution. Temporal retinal explants were treated with 2.0 μg/ml ephrin-A2 for the indicated times, fixed and then F-actin was labeled with Alexa Fluor 488-phalloidin. Total growth cone F-actin and the central vs. peripheral distributions of F-actin were quantified, as described in Materials and Methods, and as illustrated in panel **A'**. **A**. Representative images of F-actin distribution in control and ephrin-A2-treated growth cones. **B**. Integrated total F-actin staining in growth cones treated with ephrin-A2 for the indicated times. **C**. Relative distribution of F-actin into peripheral and central regions of growth cones. Statistical significance was determined using Student's *t* test. Data are means ± SEM; **P*<0.05, ***P*<0.01, ****P*<0.001. Scale bar 10 μm.

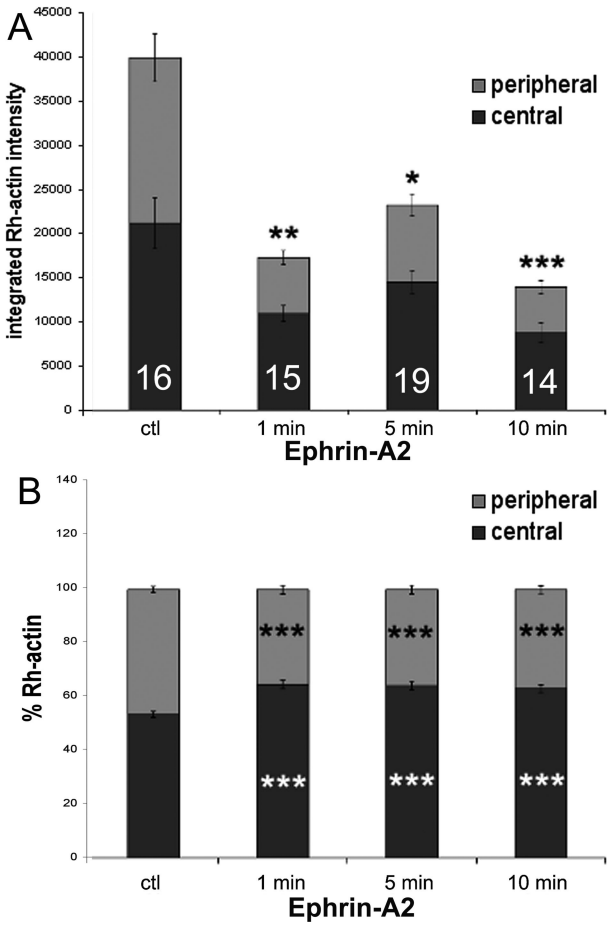

Figure 3.

Ephrin-A2 reduces free F-actin barbed ends and shifts barbed ends distribution. Temporal retinal explants were treated with 2.0 μg/ml ephrin-A2 for the indicated times, then processed to label F-actin free barbed ends, as described in Marsick et al. (2010). Total rhodamine-actin labeling and the central vs. peripheral distribution of Rhodamine-actin were quantified as described in Materials and Methods. **A**. Integrated total labeling of F-actin free barbed ends with rhodamine-actin. **B**. Relative distribution of total rhodamine-actin labeling into peripheral and central growth cone regions. . Statistical significance was determined using Student's *t* test. Data are means ± SEM; **P*<0.05, ***P*<0.01, ****P*<0.001.

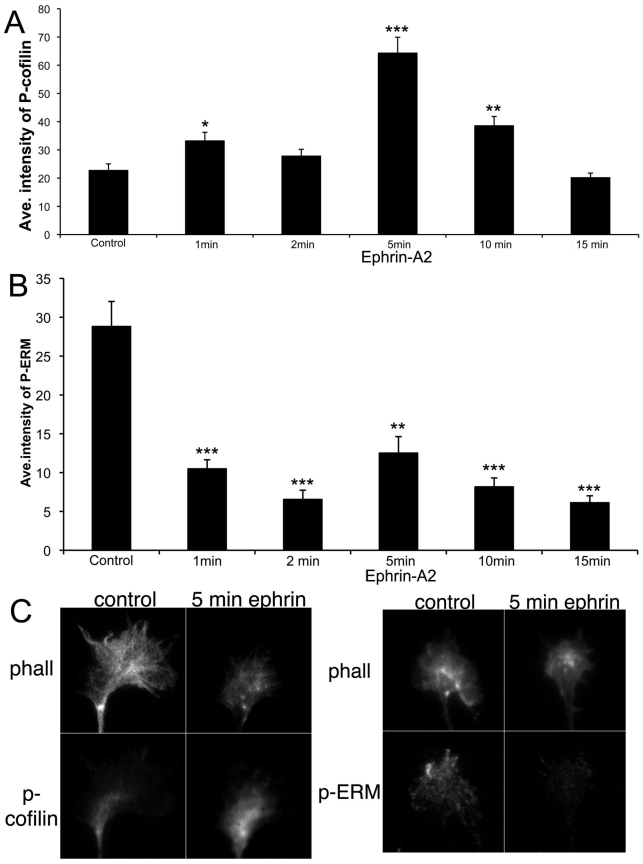

Figure 4.

Ephrin-A2 increases cofilin phosphorylation and decreases ERM phosphorylation. Temporal retinal explants were treated with 2.0 μg/ml ephrin-A2 for the indicated times, fixed and them immunocytochemically labeled for P-cofilin or P-ERM and fluorescent phalloidin. Mean staining intensity for P-cofilin and P-ERM were quantified, as described in Materials and Methods. **A**. Mean growth cone staining for P-cofilin after ephrin-A2 treatment for the indicated times. **B**. Mean growth cone staining for P-ERM after ephrin-A2 treatment for the indicated times. **C**. Representative images of P-cofilin and P-ERM staining at the indicated time points. Statistical significance was determined using Student's *t* test. Data are means ± SEM; **P*<0.01, ***P*<0.001, ****P*<0.0001.

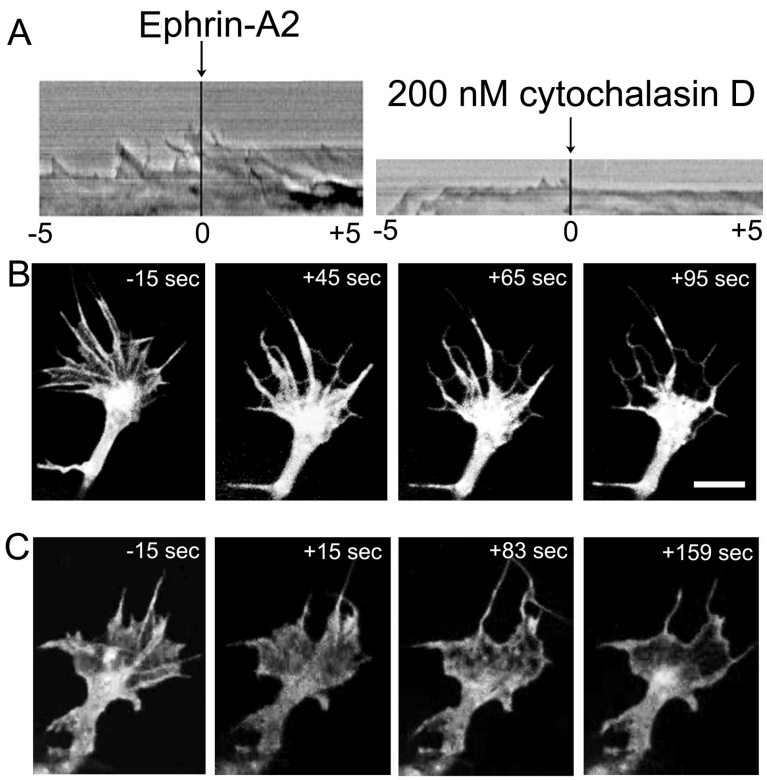

Figure 5.

Ephrin-A2 and cytochalasin D have similar effects on growth cone protrusion and actin distribution in the growth cone peripheral domain. **A**. Kymographs show the motility of growth cone leading margins before and after the addition of either 2.0 μg/ml ephrin-A2 or 200 nM cytochalasin D. These kymographs were generated from the videos shown in Supplemental Videos S2 and S3. **B**. Images of GFP-actin distribution in a growth cone treated for the indicated times with 200 nM cytochalasin D. **C**. Images of GFP-actin distribution in a growth cone treated for the indicated times with 2.0 μg/ml ephrin-A2. Scale bar 10 μm.

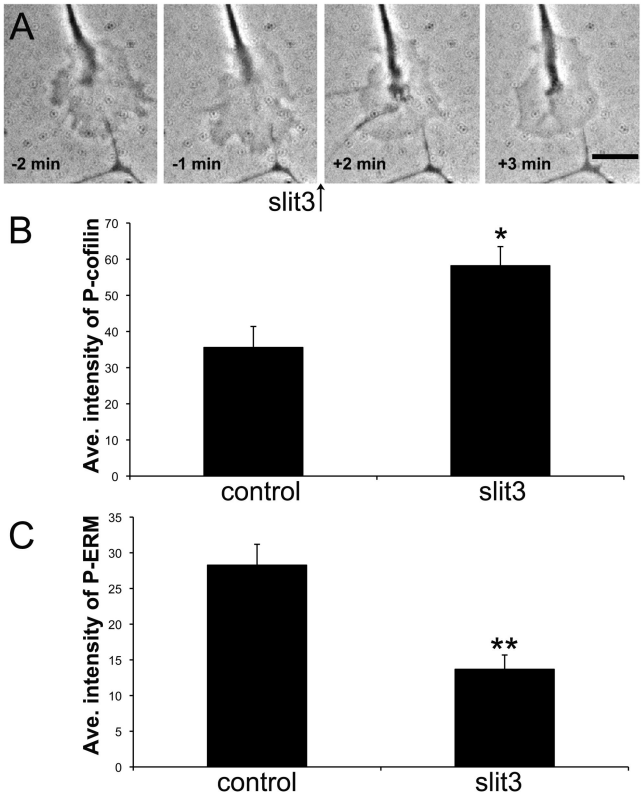

Figure 6.

Slit3 stops growth cone protrusion, increases cofilin phosphorylation and decreases ERM phosphorylation. Temporal retinal explants were treated with 2.0 μg/ml slit3 for 10 min, fixed and them immunocytochemically labeled for P-cofilin or P-ERM and fluorescent phalloidin. Mean staining intensity for P-cofilin and P-ERM were quantified, as described in Materials and Methods. **A**. Phase contrast images of a growth cone treated with slit3 for the indicated times. These images are from the sequence shown in Supplemental Video S4. **B**. Mean growth cone staining for P-cofilin. **C**. Mean growth cone staining for P-ERM. . Statistical significance was determined using Student's *t* test. Data are means ± SEM; **P*<0.01, ***P*<0.001. Scale bar 10 μm.